PAPYRUS: one year of on-sky operations

Romain Fetick, Vincent Chambouleyron, Edouard Muslimov, Idir Boudjema, Arnaud Striffling, Mahawa Cisse, Cedric Taissir Heritier, Felipe Pedreros Bustos, Esther Soria Hernández, Jacob Taylor, et al.

AO4ELT7 - June 2023 - Avignon

PAPYRUS: one year of on-sky operations

Romain JL Fétick[a,b], Vincent Chambouleyron[c], Eduard Muslimov[d], Idir Boudjema[b,e], Arnaud Striffling[a,b], Mahawa Cissé[a,b], Cédric Taissir Héritier[a,b], Felipe Pedreros[f], Esther Soria[g], Jacob Taylor[h], François Leroux[b], Raissa Camelo[b,i], Pierre Jouve[a,b], Nicolas Levraud[a,b], Jérome Schmitt[j], Jean-François Sauvage[a,b], Bruno Martin[e], Kacem El-Hadi[b], Julien Charton[e], Benoit Neichel[b], and Thierry Fusco[a,b]

[a]ONERA, DOTA, ONERA, F-13661 Salon cx Air – France
[b]Aix Marseille University, CNRS, CNES, LAM, Marseille, France
[c]University of California Santa Cruz, USA
[d]NOVA Optical IR Instrumentation Group, Dwingeloo, Netherlands
[e]ALPAO, Montbonnot-Saint-Martin, France
[f]European Southern Observatory, Germany
[g]Instituto de Astrofisica de Canarias
[h]Dunlap Institute for Astronomy & Astrophysics, Toronto, Canada
[i]SpaceAble, France
[j]Observatoire de Haute Provence, OHP, France

ABSTRACT

The PAPYRUS adaptive optics (AO) bench has been developed to test and maturate new concepts of wavefront sensors (WFS), control strategies and dedicated hardware such as cameras and deformable mirrors. The bench will serve as a pathfinder to the challenging AO systems for the upcoming Extremely Large Telescopes (ELTs). Moreover the bench has already been used as a pedagogical tool to teach adaptive optics to PhD and master students.

PAPYRUS is made of a modulated pyramid WFS working in the visible band, an EMCCD wavefront sensing camera and a 17×17 deformable mirror. The bench is installed on the T152 (1.52 m diameter) telescope at Observatoire de Haute Provence (OHP, France) since June 2022. Here we summarise the performance of the bench and the lessons learnt after one year of on-sky operations with the pyramid WFS.

Note: the author list is only indicative, all authors contributed to the project. Contact: romain.fetick@onera.fr

Keywords: adaptive optics, wavefront sensor, optical gain

1. INTRODUCTION

1.1 Observing conditions at OHP

The Observatoire de Haute Provence (OHP) is located in the South-East of France, at an altitude of 650 m. The weather is cloudy approximately 20% of the nights [13]. The median seeing ranges from 2 arcsec to 3 arcsec, with 95% of the clear nights being below 4 arcsec (all seeing values are given at 500 nm).

1.2 The T152 telescope

The T152 telescope at Observatoire de Haute Provence (OHP) has a primary mirror diameter of $D = 1.52$ m, a central obstruction of 33% of the diameter, and is built in a Cassegrain optical configuration. It is supported on an equatorial mount and the beam is available at two Coude focus with a ratio $F/D = 28$. The selection of the Coude focus is made with a flat mirror, to switch between the AURELIE spectrograph and the PAPYRUS AO bench. This telescope is available approximately 200 nights per year, allowing easy access and operations for the PAPYRUS bench.

The telescope is made of four mirrors with a reflectivity of 88% each, so the global transmission is about 50%. The main drawback of the telescope is a pointing accuracy of approximately ± 2 arcmin, and a drift on the right ascension axis while tracking that may vary according to the azimuthal orientation of the telescope with respect to the meridian.

2. DESIGN OF THE BENCH

The wavelength of the calibration laser of the Papyrus AO bench is $\lambda = 635$ nm. The scientific camera is a Hamamatsu OCRA Flash 4.0 that works in the visible, with a filter centred on the same wavelength. The WFS camera is broadband visible between $450 - 850$ nm. Consequently, all across this article, we use $\lambda = 635$ nm as the reference wavelength for expressing the r_0 and performances since it is relevant for both wavefront sensing and science cameras.

2.1 Deformable mirror and fitting error

The deformable mirror (DM) from the ALPAO company is made of 241 actuators, set on a cartesian grid 17×17. The edge actuators are mostly masked by the DM cover of the manufacturer. Moreover our optical design is defined such as the telescope pupil projected onto the DM is slightly smaller than the DM reflective area to ensure that all the T152 pupil is correctly seen by the AO system. The ratio of the diameters expressed in the same pupil plane is $D_{\mathrm{DM}}/D_{\mathrm{T152}} = 1.1$. All effects included, this translates into an equivalent 15×15 DM onsky, with a pitch onsky being $d = D_{\mathrm{T152}}/N_{\mathrm{act}} = 152/15 \simeq 10$ cm. The seeing at OHP being around 2 arcsec, the Fried parameter at $\lambda = 635$ nm is $r_{0,\lambda 635} = 6.5$ cm. The associated so-called fitting error is

$$\sigma^2_{\mathrm{fitting}} = 0.27 \left(\frac{d}{r_0} \right)^{5/3} \simeq 0.63\,\mathrm{rad}^2 \tag{1}$$

Using the Marechal approximation, the maximum Strehl ratio in median seeing conditions is

$$S_{\mathrm{max},\lambda 635} = e^{-\sigma^2_{\mathrm{fitting}}} = 53\% \tag{2}$$

2.2 WFS camera and noise error

The WFS camera is a OCAM2K from First Light Imaging company. This camera is an EMCCD operating in the broadband visible wavelengths. It has high quantum efficiency and a low electronic noise when using the electron multiplication (EM) mode. However our camera is the very first prototype of OCAM2K, and thus does not benefit from the commercialised cameras improved features. The EM gain of our camera is currently locked to 300 instead of 1000, and the pixel 2×2 binning is inactivated. Thus we suffer from higher noise than usual, limiting our performances in guide star magnitude. By optical design, the pupils are highly oversampled with respect to the DM. Indeed the DM is made of 17 actuators (15 equivalent actuators onsky), whereas a pupil stands on 70 pixels large on the WFS camera. The oversampling is thus a factor of 4 on each direction. We are consequently able to distinguish fine structures in the pupil plane (thin T152 spiders, turbulence high spatial frequencies), at the disadvantage of an increased read-out noise and pixel transfer and processing time.

The AO bench and telescope transmission from the entrance pupil up to WFS camera is of the order of 5% all effects included. This value is consistent with our transmission estimations: 50% from the telescope itself, 25% from the two consecutive beam splitter, and the remaining transmission drop might be due to Papyrus optics (four OAPs, flip mirror, slow tip-tilt, DM, modulator, lenses) as shown in Section 2.5

With the current configuration, the maximum reachable magnitude is 5.5 at $F = 500$ Hz. It is planned to update both the WFS camera and the AO bench design to improve the SNR and close on fainter stars. The actual beam-splitter between the science branch and WFS branch will be replaced by a visible vs IR dichroic, and the second beam splitter between the WFS camera and the Gain Sensing Camera (GSC) has a $50\% - 50\%$ splitting ratio that could be fine tuned (expected 90% for the WFS and 10% for the GSC). The corresponding improvement will be approximately 2 magnitudes for the sole bench design modifications. Updates on the WFS camera (higher EM gain and lower number of pixels in the pupil) will also provide better SNR and help to close on fainter stars, with a rough estimation of $1 - 2$ extra magnitudes.

2.3 Real time controllers and temporal error

The PAPYRUS bench can be run from two different computers, the homemade PAPYRUS-RTC and the industrial ALPAO-RTC. The PAPYRUS-RTC itself can be run on two different RTC softwares, making up to 3 different RTC options:

- PAPYRUS-RTC running Matlab software and Windows OS (500 Hz). This software can easily be updated, it consequently perfectly matches our requirements for a modular AO bench. This has been the main RTC for our tests and performances onsky so far.
- PAPYRUS-RTC running the CHAI RTC, an adaptive optics plugin developed for the image processing software MILK [1]. CHAI is a high performance RTC software, written in C/C++, that was originally developed for the MAPS AO system on the MMT [10]. It has been recently adapted for PAPYRUS and some initial tests have been run on internal calibration source. This solution is compatible (hardware and drivers) with ELT/Harmoni RTC and might be pushed forward for future operations of Papyrus.
- ALPAO-RTC running ALPAO software (1.5 kHz). It has been operated at full speed on sky. However it still requires some software updates on calibration and modal control before being perfectly operational.

The PAPYRUS-RTC with Matlab software is the one giving both good performances and the one we understand more the critical steps for running an AO loop. We thus use it for commissioning operations even though it is limited to a loop frequency of 500 Hz. Other RTCs will be used more often in the future. The error transfer function (ETF) of the homemade PAPYRUS RTC is shown on Figure 1. It fits the theory with good agreement and allows to determine a delay of 0.8 frame (at 500 Hz) caused by pixel transfer and RTC operations.

For an integrator control law, the temporal bandwidth of the system is given by

$$B = \frac{F}{2\pi}\sqrt{\frac{g}{1 + 2\tau F}} \tag{3}$$

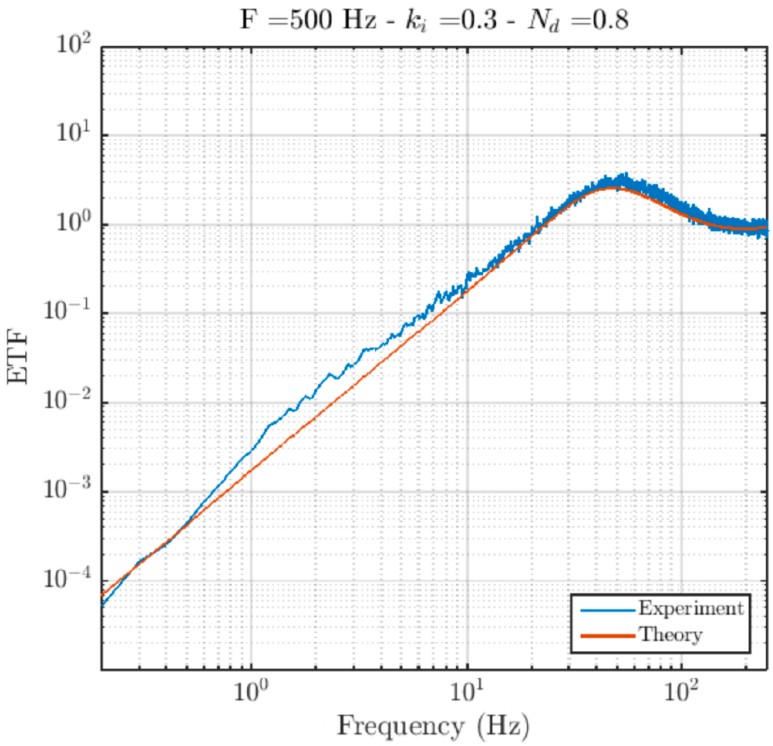

Figure 1. Error transfer function (ETF) of the Papyrus bench using the PAPYRUS homemade RTC. Experimental data is plotted in blue, theoretical function in orange.

where F is the loop frequency, g the integrator gain and τ the loop delay. For our system running at $F = 500$ Hz, a loop gain $g = 0.3$ and 1 frame delay for RTC computations (plus one frame of integration), we compute a temporal bandwidth $B = 25$ Hz. The temporal error writes [4]

$$\sigma^2_{\text{temporal}} = 0.04 \left(\frac{V}{DB}\right)^2 \left(\frac{D}{r_0}\right)^{5/3} \sum_{n=1}^{N_r} (n+1)^{-2/3} \tag{4}$$

where V is the wind speed and N_r the number of radial corrected modes. In our case, we correct for 190 modes, corresponding to approximately $N_r = 18$ radial modes. For our system, the formula gives $\sigma^2_{\text{temporal}} \simeq 0.033\, V^2$, where V is expressed in meter per second. The hypothesis behind the computation is that the system works in the linear regime, it thus ignores the pyramid optical gains. The formula above is consequently a lower limit on the phase variance, so induces a upper limit on the Strehl ratio.

2.4 Expected performances

We use the AOERROR [8] tool, written in Python, to derive the Papyrus performances with respect to the observing conditions. The code generates the power spectral density (PSD) of the AO corrected phase and computes the theoretical PSF according to the formalism developed in [14]. The code also takes into account the so-called pyramid optical gains (OG), which are computed using the convolutional formalism [6, 5].

Figure 2 shows the results of the simulated PSF for different wind speeds and a seeing set at 2 arcsec in a noise-free WFS regime. The left graphs shows the dramatic decrease of Strehl when the wind speed increases as our system runs at $F = 500$ Hz. The optical gains are responsible for a loss of Strehl up to 10%. This gives margin for performance increase in the future compensation of the optical gains [15].

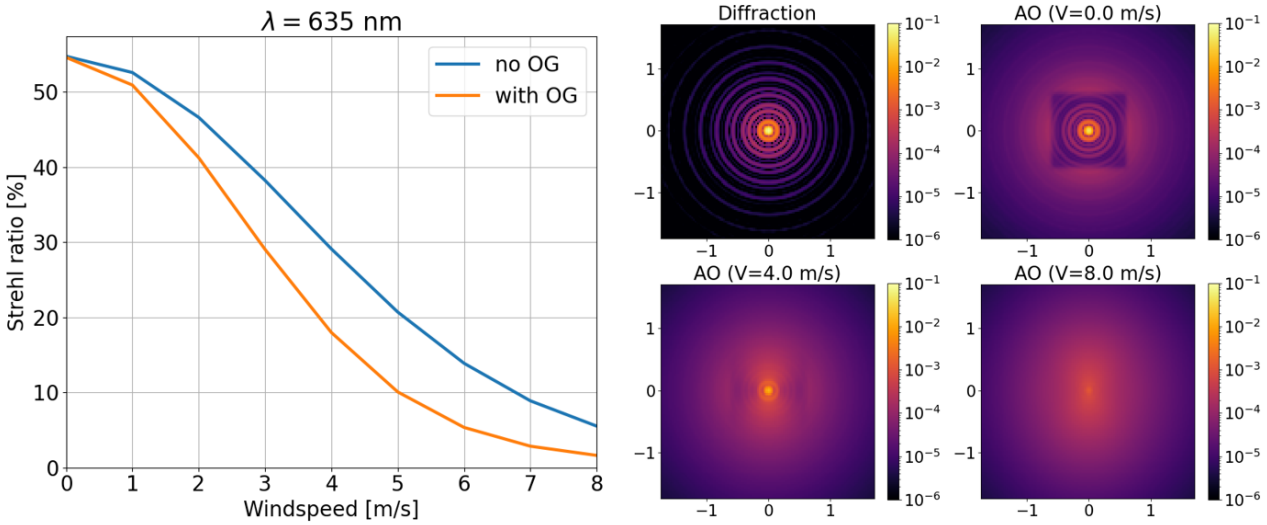

Figure 2. Simulation of Papyrus performances at $\lambda = 635$ nm with a 2 arcsec seeing conditions and infinite SNR. The four images on the right side show the PSF at diffraction limit (no atmosphere), $V = 0$ m/s (fitting error only, best performance), $V = 4$ m/s (moderate wind) and $V = 8$ m/s (strong wind). X and Y axes of the four PSF images are graduated in arcsec. All the AO computed PSF include the optical gains.

2.5 Optical design

The optical design of PAPYRUS is shown on the schematics of Figure 3, a more precise design can be found in [12]. The bench is made of four different parts: the common path, the calibration path, the wavefront sensing path and the science path.

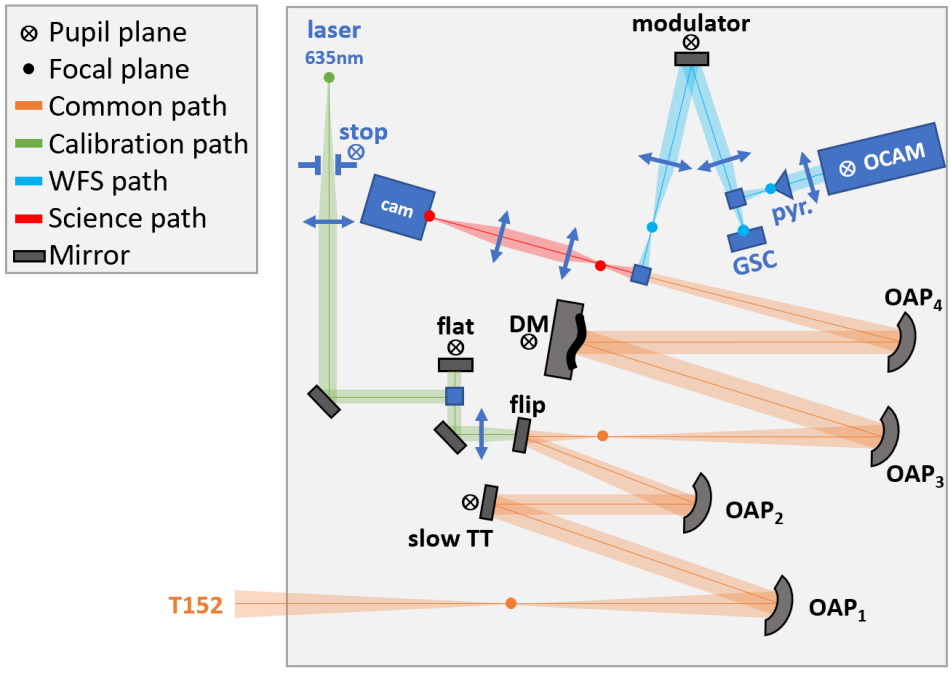

Figure 3. Schematics of the PAPYRUS optical bench

The common path is made of reflexive components only to avoid chromatic effects and to fold the beam for instrument compacity. There are four off the shelf off-axis parabolas (OAP) to reshape the beam to the two different pupil planes which are the slow tip-tilt and the deformable mirror. One component of the common path is a flip (flat) mirror. It allows to select between the telescope light for onsky operations or the laser $\lambda = 635$ nm light for calibration. The calibration beam illuminates the full aperture of the deformable mirror, so the DM reflective area is the pupil, limited by the manufacturer cover. However the T152 pupil projected on the DM is smaller of a factor of 1.1 to compensate for possible pupil misalignment or movements. Fortunately, the telescope pupil is stable, since we didn't see any pupil translation with respect to the telescope position. However the pupil is naturally rotating due to the telescope optical design, we didn't notice any effect on the AO control since the spiders are much smaller than the DM pitch on-sky.

The common path ends on a 50/50 visible beam splitter to separate the light between the science path and the WFS path. This beam splitter will soon be changed for a visible/IR dichroic to perform science in the IR and collect more visible photons onto the WFS. For this last year of operation, the science has been performed in the visible.

Finally, the WFS path uses a modulator, followed by another 50/50 visible beam splitter. Half of the flux goes to the pyramid and then to the OCAM2K camera. The other half is sent on the gain sensing camera (GSC) [3, 15]. This camera sees the actual modulated PSF, as seen by the pyramid, it will allow for frame-to-frame optical gain tracking and compensation [15].

3. ON-SKY RESULTS

The PAPYRUS bench has been installed at the T152 since June 2022 and provided AO corrected images in the visible since then. For on sky operations on stars (simple or binaries), the modulation radius is usually set between $5\lambda/D$ and $7\lambda/D$.

The PAPYRUS bench provides a set of data associated to each observation. All these data are used to estimate observing conditions and to correlate them with performances of the AO loop. These data include:

- WFS frames (see Fig. 4). These images cannot be saved at $F = 500$ Hz due to extra load on the RTC that slows down the loop.
- Calibration data, including calibration matrix, DM flattening coefficients (to compensate for internal aberrations), pupil binary mask to extract slopes from WFS images.
- DM coefficients. These coefficients can be saved at loop speed, allowing to reconstruct the DM phase afterwards.
- Gain Sensing camera frames (see Fig. 4)
- PSF on the scientific camera (see Fig. 4)

3.1 Performances (statistics and best case)

The seeing at OHP was monitored using the external COLIBRI seeing monitor for a short period (up to June 2023) and in a long term with the IRIS seeing monitor [9]. We compare this external data with the PAPYRUS estimations. Our estimations are based on PSF fitting method with PSF theoretical models in open loop or closed loop [7]. This fitting allows to extract the r_0 parameter, given at the scientific camera wavelength and line-of-sight. Figure 5 shows seeing estimation with different methods. Whereas the COLIBRI seeing shows large variations, the PAPYRUS one is more stable. PAPYRUS seeing estimation is slightly higher in average. We believe the T152 telescope and dome might induce extra local turbulence that impact our observations.

Figure 6 shows the Strehl ratio observed on the long-exposure AO corrected PSF with respect to the PAPYRUS estimated r_0. On this dataset, the Strehl ratio ranges from 10% to 33%. This last value is the best Strehl ratio we obtained on PAPYRUS so far (see Figure 7), as the result of good seeing conditions according to the estimated $r_0 = 7.2$ cm (at 635nm) and supposedly quite low wind. Consequently both the fitting error and temporal error

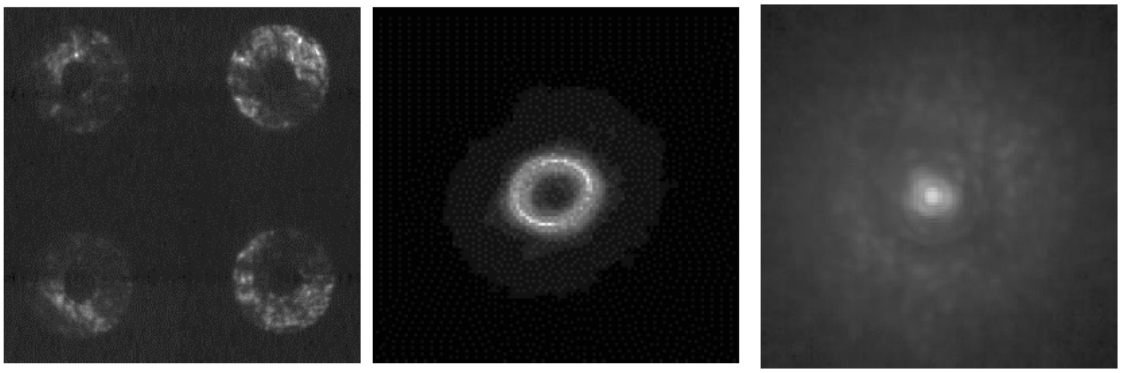

Figure 4. Typical images obtained with PAPYRUS. From left to right: T152 pupils on the OCAM2K, modulated PSF on the GSC, PSF in the scientific branch (log scale and cropped to see the central peak, first ring and correction area).

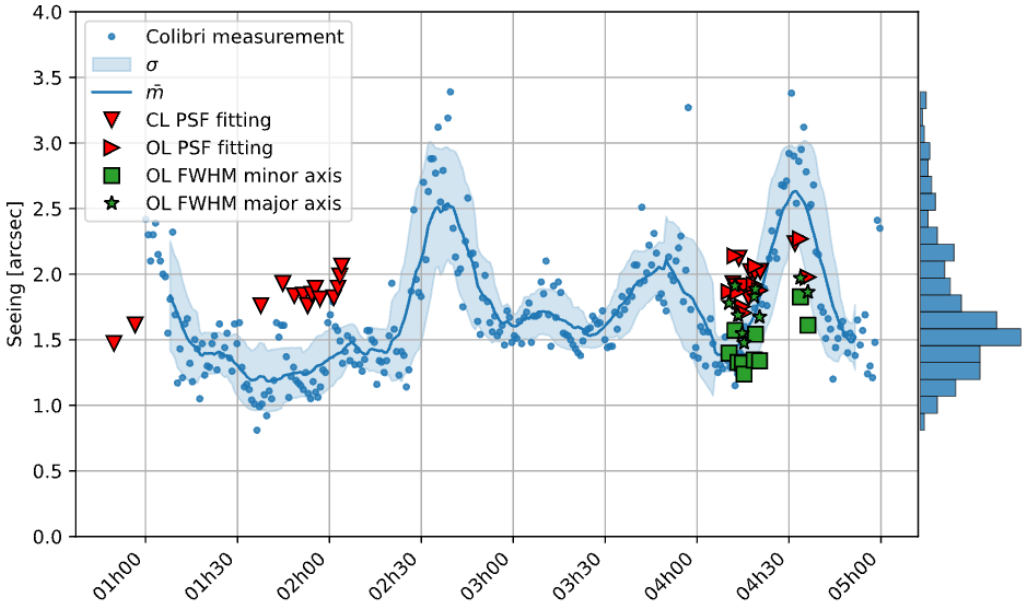

Figure 5. Seeing estimations at OHP on May 26th, 2023. Blue dataset comes from the COLIBRI instrument that was present at OHP at this date, red and green symbols are PAPYRUS estimations from the PSF image, using PSF fitting and FWHM respectively to estimate the seeing.

(discussed in the previous section) are low. All the measured data are located in between the theoretical Strehl curves for a wind speed of 5 m/s and 9 m/s. However these curves are the direct computation of equations 2 and 4, and don't take into account the optical gain. In the presence of optical gain, the actual wind speed might then slightly smaller than the one from the equations to produce a similar Strehl ratio. Moreover the Maréchal approximation is used to plot the theoretical curves, whereas this approximation is known to underestimate the Strehl ratio in poor conditions.

3.2 Jitter

The PSF jitter is estimated by center of gravity on a cube of short-exposure PSF. The cube is made of 500 consecutive images with an exposure time of 10 ms each. Figure 8 shows that we achieved a jitter of approximately $0.1\,\lambda_{635}/D$ RMS. This result gives us confidence in the possibility to inject post-AO light into an optical fiber, especially for an infrared spectrometer working in H or K band.

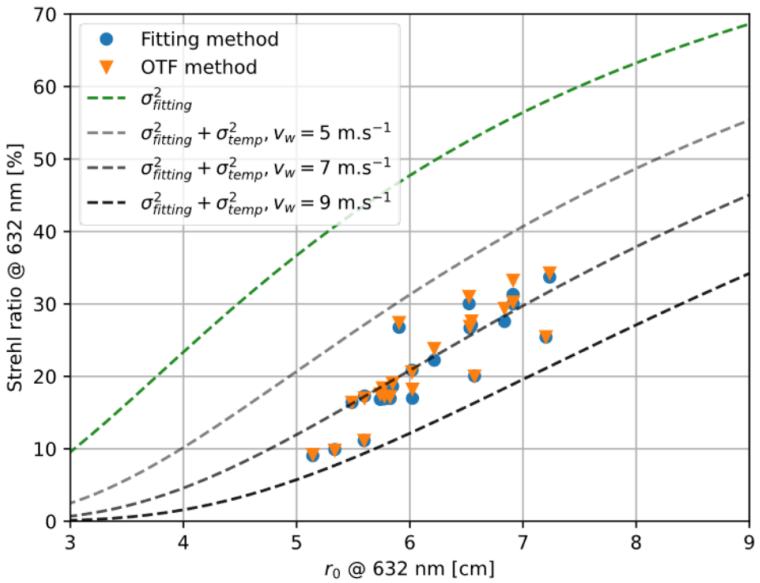

Figure 6. Strehl computed from PAPYRUS PSF as function of the estimated r_0 (symbols). The data is compared with theoretical curves, without including optical gains, for different windspeed conditions (dashed lines).

3.3 Extended object: Mars

On September 12th, 2022 we closed the AO loop on planet Mars to test the capabilities of the pyramid WFS on extended objects. Indeed at that time, Mars was close to Earth, with an apparent diameter of 11 arcsec. This is 128 times the diffraction size for both the science and WFS since the diffraction size is $\lambda_{635}/D = 86$ mas. For such a large object we modulated in calibration with a radius of 15 λ_{635}/D. This modulation is much smaller than the natural modulation induced by the size of the object, but we were unable to modulate to a higher amplitude because of the limited range of the modulating mirror. When observing Mars, we stop the modulation and use the natural modulation of the wavefront induced by the extended object (incoherent light coming from different spatial positions). However, there was still a factor of 4 between the Mars size and the calibration modulation diameter that we could not compensate and that might have introduced extra optical gains, and consequently lowered the performances of our AO system. The open loop and closed loop data is shown on Figure 9.

Moreover we performed deconvolution using the MISTRAL algorithm [11]. The goal of the deconvolution is to restore the original spatial frequencies that were present in the image but attenuated due to the PSF blurring. The pyramid WFS associated with deconvolution is thus able to restore finest details and sharp edges (Fig. 9, right plot) on resolved objects.

Finally, we plan to compensate soon the optical gains on the PAPYRUS bench, this might increase further the performances of the AO system on extended objects.

4. CONCLUSION

After one year of operations, the PAPYRUS bench has demonstrated its capability to perform AO with a visible pyramid WFS. It reaches up to 30% of Strehl ratio at $\lambda = 635$ nm when closing on a bright star. We also closed the AO loop on a very extended object.

The results match our expectations of the bench performances from pre-design and simulations. We are now moving forward to a more exploratory path for PAPYRUS future developments. Among others, we are interested in fully compensating the optical gains and managing extended objects with the pyramid wavefront sensor with the goal of increasing the performances of pyramid WFS systems.

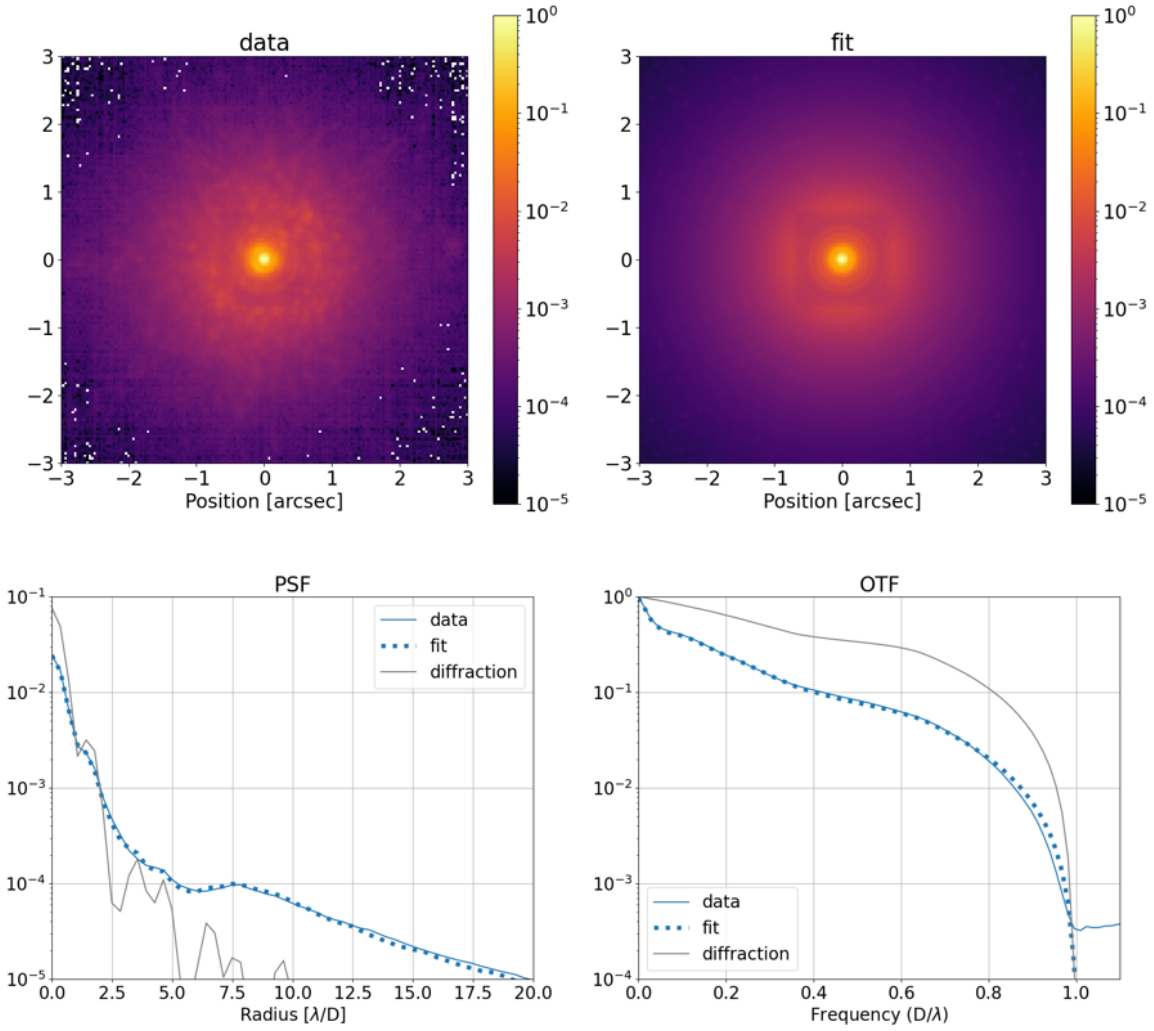

Figure 7. Best Strehl ratio case of PAPYRUS of $S_r = 33\%$, obtained on May 26th, 2023. Top row show the PSF and the fit with a theoretical model. Bottom row show the PSF and OTF circular averages.

Moreover, a second AO stage including a double Zernike wavefront sensor is in conception phase. PAPYRUS will thus test innovative and highly sensitive wavefront sensors in the upcoming years to prepare second-generation instruments on ELT-like telescopes.

On the instrument coupling side, a scientific IR branch will be designed and implemented in order to couple an optical fibre to inject light of binary star into the VIPA high-resolution spectrometer [2]. This collaboration will be fruitful both to test the spectrometer after an AO system, and to maintain non-common-path aberrations with Fourier filtering wavefront sensors for next generation of extreme adaptive optics.

ACKNOWLEDGMENTS

This work benefited from the support of the the French National Research Agency (ANR) with WOLF (ANR-18-CE31-0018), APPLY (ANR-19-CE31-0011) and LabEx FOCUS (ANR-11-LABX-0013); the Programme Investissement Avenir F-CELT (ANR-21-ESRE-0008), the Action Spécifique Haute Résolution Angulaire (ASHRA) of CNRS/INSU co-funded by CNES, the ECOS-CONYCIT France-Chile cooperation (C20E02), the ORP-H2020 Framework Programme of the European Commission's (Grant number 101004719), STIC AmSud (21-STIC-09),

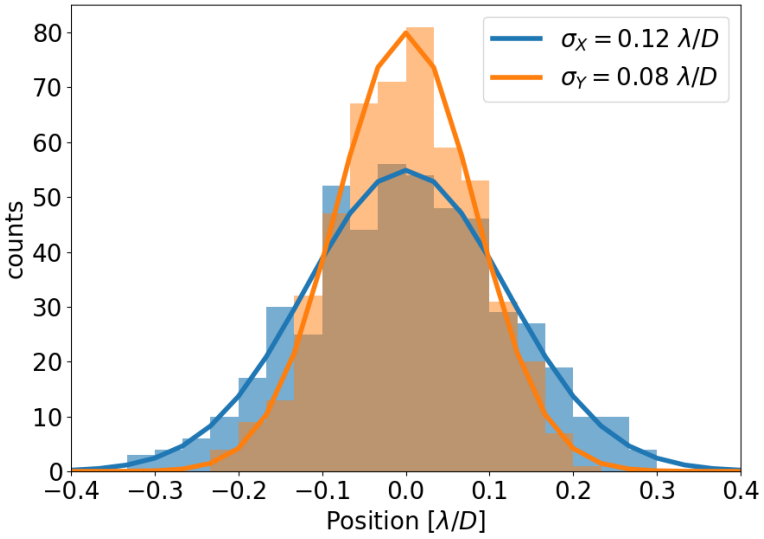

Figure 8. Jitter estimation on PAPYRUS, at $\lambda = 635$ nm. The two datasets, of different colors on the figure, correspond to the scientific camera horizontal and vertical axis.

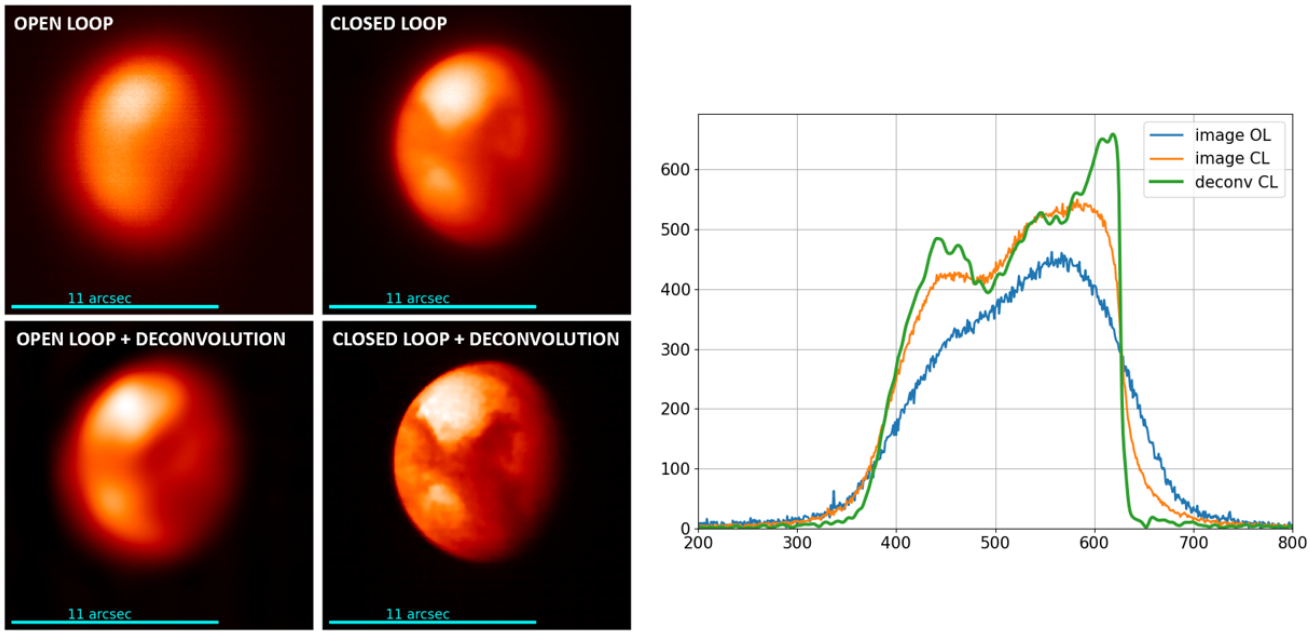

Figure 9. Left images: Mars observed by PAPYRUS on September 12th, 2022. Right plot: cut view along the diameter of Mars for the open loop image (blue), closed loop image (orange) and closed loop deconvolution (green). X axis is graduated in pixels, and Y axis in arbitrary unit.

the Région Sud and the french government under the France 2030 investment plan, as part of the Initiative d'Excellence d'Aix-Marseille Université -A*MIDEX, program number AMX-22-RE-AB-151.

References

[1] URL: https://milk-org.github.io/milk/.

[2] Guillaume Bourdarot et al. “Experimental test of a 40 cm-long R= 100 000 spectrometer for exoplanet characterisation”. In: *Ground-based and Airborne Instrumentation for Astronomy VII*. Vol. 10702. SPIE. 2018, pp. 1798–1809.

[3] Vincent Chambouleyron et al. “Focal-plane-assisted pyramid wavefront sensor: Enabling frame-by-frame optical gain tracking”. In: *Astronomy & Astrophysics* 649 (2021), A70.

[4] Jean-Marc Conan. “Etude de la correction partielle en optique adaptative”. PhD thesis. Paris 11, 1994.

[5] Olivier Fauvarque. “Optimisation des analyseurs de front d’onde à filtrage optique de Fourier”. PhD thesis. Aix-Marseille, 2017.

[6] Olivier Fauvarque et al. “General formalism for Fourier-based wave front sensing”. In: *Optica* 3.12 (Dec. 2016), pp. 1440–1452. DOI: 10.1364/OPTICA.3.001440.

[7] RJL Fétick et al. “Physics-based model of the adaptive-optics-corrected point spread function-applications to the sphere/zimpol and muse instruments”. In: *Astronomy & Astrophysics* 628 (2019), A99.

[8] *Including the pyramid optical gains into analytical models*. 2023.

[9] https://iris.lam.fr/statut-observatoire/conditions-observations/.

[10] Manny Montoya et al. “Status update for MAPS, the MMT AO exoPlanet characterization System”. In: *Adaptive Optics Systems VIII*. Vol. 12185. International Society for Optics and Photonics. SPIE, 2022, 121856S. DOI: 10.1117/12.2619434. URL: https://doi.org/10.1117/12.2619434.

[11] Laurent M Mugnier, Thierry Fusco, and Jean-Marc Conan. “MISTRAL: a myopic edge-preserving image restoration method, with application to astronomical adaptive-optics-corrected long-exposure images”. In: *JOSA A* 21.10 (2004), pp. 1841–1854.

[12] Eduard Muslimov et al. “Current status of PAPYRUS: the pyramid based adaptive optics system at LAM/OHP”. In: *Optical Instrument Science, Technology, and Applications II*. Vol. 11876. SPIE. 2021, pp. 56–68.

[13] http://www.obs-hp.fr/climatologie.shtml.

[14] François Roddier. “V the effects of atmospheric turbulence in optical astronomy”. In: *Progress in optics*. Vol. 19. Elsevier, 1981, pp. 281–376.

[15] Arnaud Striffling et al. “Toward the full control of NCPA with the pyramid wavefront sensor: mastering the optical gains”. In: *AO4ELT-7 proceedings* (2023).